Preparation of doping titania antibacterial powder by ultrasonic spray pyrolysis

WEI Shun-wen(韦顺文)[1], PENG Bing(彭 兵)[1], CHAI Li-yuan(柴立元)[1],
LIU Yun-chao(刘云超)[1], LI Zhu-ying(李竹英)[2]

1. School of Metallurgical Science and Engineering, Central South University, Changsha 410083, China;
2. Yiwu Bureau of Quality and Technical Supervision, Yiwu 322000, China

Abstract: Doping titania powders were synthesized by ultrasonic spray pyrolysis method from an aqueous solution containing H_2TiF_6 and $AgNO_3$. The effects of the processing parameters on particle size distribution, structure, and morphology of doping particles were investigated. The results show that aggregation-free spherical particles with average diameter of 200−600 nm are obtained and the particle size of the powder can be controlled by adjusting the concentration of solution. The experimental approach indicates that the size and the value of standard deviation of particle size increase from 210 nm to 450 nm and from 0.46 to 0.73 respectively with the increase of the titanic ion concentration from 0.05 to 0.4 mol/L. Composite $TiOF_2$ is obtained when the pyrolysis temperature is set to be 400 ℃. With increasing pyrolysis temperature from 400 ℃ to 800 ℃, the crystal size of titania powders increases from 14.1 to 26.5 nm and $TiOF_2$ content of powder decreases dramatically. The property of ion released from powder is affected significantly by the pyrolysis temperature, and the amount of fluorine ion and silver ion released from powder decrease with increasing pyrolysis temperature. The optical property of doping titania powders is not affected by pyrolysis temperature. Antibacterial test results show that composite powders containing more fluorine ions exhibit stronger antibacterial activity against *E.coli*.

Key words: doping; titania; spray pyrolysis; antibacterial powder

1 Introduction

Titanium dioxide is an attractive photocatalyst and has been applied widely[1−2]. Due to its photosemi-conductor properties[3], titanium dioxide may find an application as an antibacterial agent[4] for the decomposition of organism. But its photocatalysis is only activated by UV light and only 5% of solar spectrum is used[5]. In order to enhance the quantum efficiency of the titanium dioxide catalyst, many efforts have been made to eliminate the fast geminate recombination of electron-hole pairs produced by the photon excitation. The addition of noble metal such as silver, gold and platinum is one of the methods to improve the photocatalytic activity[6−7]. When titanium dioxide is doped by silver ion, composite has a good antibacterial activity even without the presence of light. But silver ion is unstable and easily transformed to black metallic silver or brown silver oxide during illumination or thermal treatment. The color stability of silver ion in titania is affected by many factors[8], such as the ligand, dispersion of silver ion, particle size and structure of titania. These factors are related to the preparation method, so it is very important to choose a suitable preparation route to obtain titania composite powders containing silver. Ultrasonic spray pyrolysis is one of the best methods to produce small and uniform particle, moreover, the preparation of silver-doped titania by spray pyrolysis has not been reported. Therefore, in this work, titania containing silver was prepared by spray pyrolysis method. The effects of process parameters, such as pyrolysis temperature and titanic ion concentration on the properties of doping titania particles were studied.

2 Experimental

2.1 Material preparation

A starting solution was prepared by adding silver nitrate into H_2TiF_6 solution at a constant molar ratio

0.0045 of Ag to Ti, the starting solution was diluted by water, and the titanic concentration of the starting solution was adjusted to 0.05, 0.1, 0.2 and 0.4 mol/L, respectively. Doping TiO_2 powders were synthesized by spray pyrolysis from the starting solution. The schematic drawing of ultrasonic spray pyrolysis system for doping titania powder preparation is shown in Fig.1. The starting solution was atomized by a nebulizer(the power of the nebulizer is about 80 W, 2.50 MHz); then the formed droplets carried by gas and passed through a high-temperature tube under the suction of an aspirator. The furnace temperature was set to be 500, 600, 700 and 800 ℃, respectively. The pyrolysis reaction proceeded quickly as droplets passed through the high-temperature tube. The pyrolysis reactions were as follows:
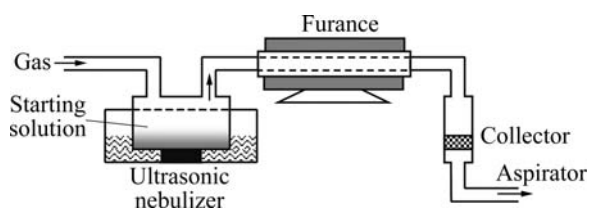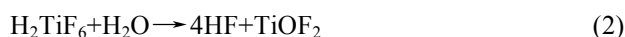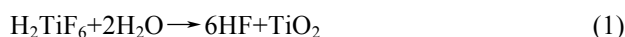
$$H_2TiF_6 + 2H_2O \longrightarrow 6HF + TiO_2 \tag{1}$$

$$H_2TiF_6 + H_2O \longrightarrow 4HF + TiOF_2 \tag{2}$$

$$TiOF_2 + H_2O \longrightarrow TiO_2 + 2HF \tag{3}$$

Fig.1 Schematic drawing of ultrasonic spray pyrolysis system

The generated powder was collected with a ceramic filter at the end of the tube.

2.2 Characterizations

The particle size distribution, specific surface area (SSA), optical property, morphology and structure of samples were measured with a laser particle size analyzer (MS−2000), low temperature gas (nitrogen) adsorption apparatus and UV-vis spectrophotometer, transmission electronic microscope(TEM), Philips PW1780 X-ray diffractometer(XRD), respectively. The crystallite sizes of anatase titania were estimated by analyzing the broadening of the (101) reflection. The average particle sizes can be calculated by Scherrer law as follows:

$$d = \frac{0.9\lambda}{\beta \cos\theta} \tag{4}$$

where λ is the wavelength of X-ray source (Cu K_α, 1.054 Å), and β is the full-width at half-maximum of the X-ray diffraction peak at the diffraction angle θ. The fraction of rutile in each sample was determined by measuring the relative XRD intensities of the anatase (101) and rutile (110) from the following equation:

$$w = 1/[1 + 0.8(I_A/I_R)] \tag{5}$$

where w is the mass fraction of rutile in the powder, while I_A and I_R are the X-ray integrated intensities of the (101) reflection of anatase and (110) reflection of rutile, respectively.

The silver release property of the particles was examined by leaching with distilled water. 2 g composite powder was added in 200 mL of distilled water in a polypropylene bottle at 37 ℃ and stirred mechanically at 120 r/min. The supernatant liquor was collected after the powder was soaked in water for 1 d and analyzed for silver ion concentration by atomic adsorption spectro-photometry (AAS) and F^- ion concentration by ion selective electrode method.

2.3 Antibacterial test

The antibacterial activity of composite powders was evaluated by measuring the minimum inhibitory concentration(MIC). The MIC of samples was defined as the lowest concentration of samples in which more than 90% bacteria could not grow. A series of broth containing samples were prepared, and the concentration of samples was adjusted to 1−10 mg/mL by diluting appropriate volume of BHI-broth. *E. coli* species was cultured in BHI-broth, and the concentration of *E.coli* inoculum was adjusted to 10^6cells/mL under microscope. Then, 1 mL *E.coli* inoculum was added to 9 mL of a series of broth containing samples, and the bacteria were cultured in the box at 37 ℃ for 48 h with gentle stirring to prevent samples from depositing. The MIC of samples was measured.

3 Results and discussion

3.1 Particle size distribution

The theoretical diameter of the droplets sprayed by ultrasonic generator can be approximately calculated using Lang's equation[8]:

$$D_d = 0.34 \times 10^6 \left(\frac{8\pi\sigma}{\rho f^2}\right)^{1/3} \tag{6}$$

where D_d is the droplet diameter (μm), σ is the solution surface tension (N/m), ρ is the solution density (g/cm³), and f is the ultrasonic frequency of the nebulizer (2.5 Hz). By considering that the nitrate salts have no influence on σ and ρ, the diameter of the droplet calculated using Eqn.(6) is 2.1 μm.

The relationship between the theoretical diameter of the doping titania particle and the droplet diameter can be describe as[8]

$$d = 10^3 \times \left(10^{-3} \times \frac{cMD_d^3}{\rho_t}\right)^{1/3} \tag{7}$$

where d is theoretical diameter of the doping titania

particle (nm), c is the concentration of titanium dioxide in the solution (mol/L), M is the molar mass of titanium dioxide (g/mol), and ρ_t is theoretical titanium dioxide density (g/cm^3). The theoretical diameters d calculated using Eqn.(7) for concentration of 0.05, 0.1, 0.2 and 0.4 mol/L are 207, 260, 328 and 414 nm, respectively. The theoretical diameter of the doping titania particle increases with increasing the concentration of titanium dioxide in the solution (c).

The particle size distribution of doping titania powder prepared at 800 ℃ is presented in Fig.2. The average size and standard deviation(D_s) of particle are shown in Fig.3. It can be seen from Fig.2 and Fig.3 that the mean size of particles and the values of D_s increase with increasing the titanic concentration of solution. When the titanic concentration is 0.05 mol/L, the particle has a narrow size distribution around 210 nm; when the titanic concentration is 0.4 mol/L, the particle has a broad size distribution around 450 nm. The increasing of D_s from 0.46 to 0.73 indicates that the uniformity of particle decreases. The change in average particle size is consistent with the theoretically calculated results.
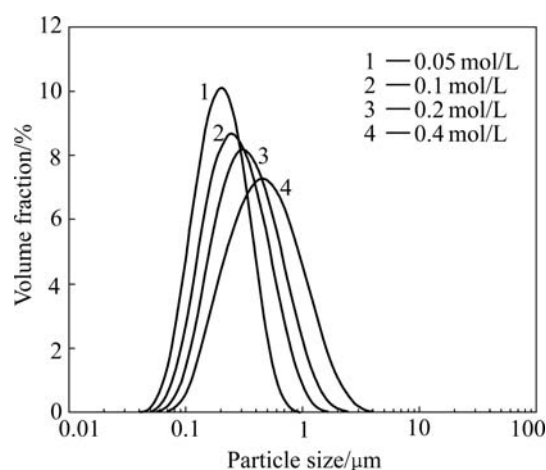

Fig.2 Particle size distribution of doping titania powders as function of Ti^{4+} concentration of solution
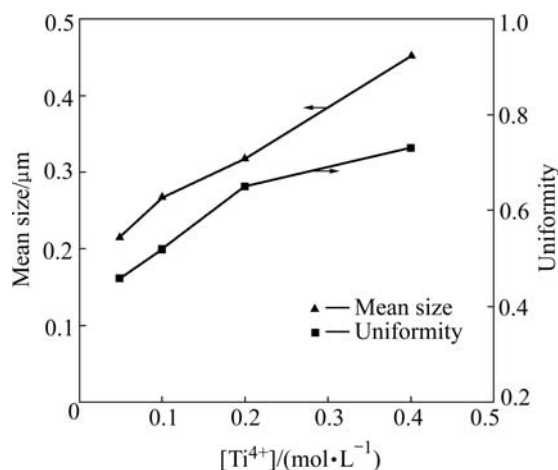
Fig.3 Mean size of particles and standard deviation as function of Ti^{4+} concentration of solution

3.2 Structure and morphology

The XRD patterns in Fig.4 indicate that the pyrolysis temperature has a great effect on the phase composition of doping titania powders. A pure anatase phase of titania was observed when the pyrolysis temperature was set between 500 and 700 ℃. Some peaks assigned to TiOF$_2$ were observed for powder prepared at 400 ℃. It can be explained that the ion radius of fluorine atom (0.133 nm) is virtually the same as the replaced oxygen atom (0.132 nm), and the fluorine atom can displace oxygen atom in TiO$_2$ matrix to form TiOF$_2$. The rutile phase appeared in composite when the pyrolysis temperature was set to be 800 ℃, but a considerable amount of anatase still remained in powder. The diffraction peaks corresponding to silver were not observed in XRD patterns for low content of silver in samples. The crystal sizes of titania calculated from the (101) peak of the XRD pattern are presented in Fig.5 and range from 14.1 to 26.5 nm, monotonically increasing with increasing pyrolysis temperature.
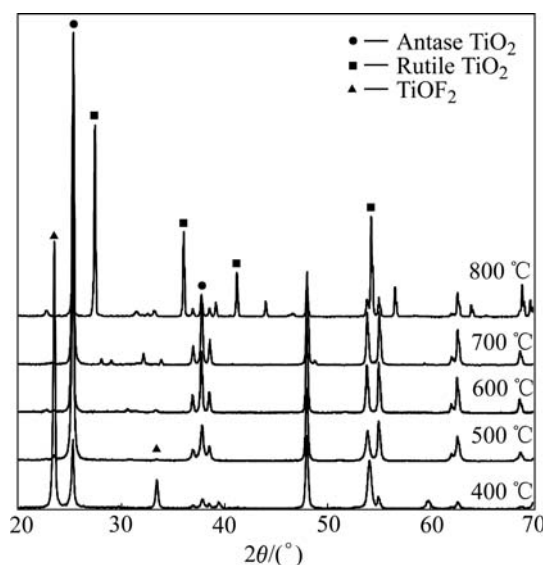

Fig.4 X-ray diffraction patterns of powders prepared at different furnace temperatures

Fig.6 shows TEM images of the doping TiO$_2$ powder prepared from solution with various titanic concentrations. It can be seen that the doping TiO$_2$ powder is aggregation-free spherical particle with an average diameter about 200−600 nm. The diameter of particle prepared from 0.05 mol/L titanic solution is smaller than that prepared from 0.4 mol/L titanic solution. The change in particle size is also consistent with theoretical calculated results.

3.3 Optical property

It is known that the electron (e$^-$) and hole (h$^+$) are generated when TiO$_2$ is exposed in UV light. With
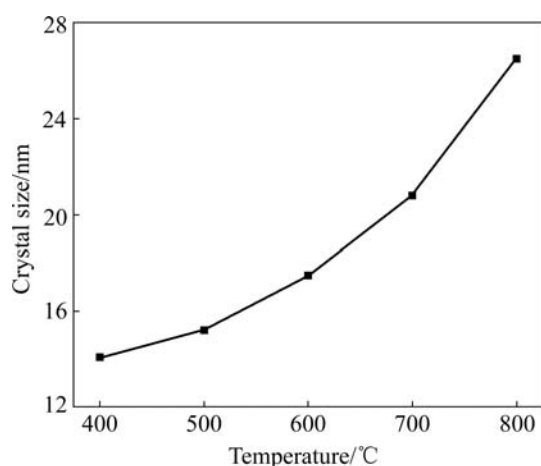
Fig.5 Effect of furnace temperature on silver-doped titania crystal sizes
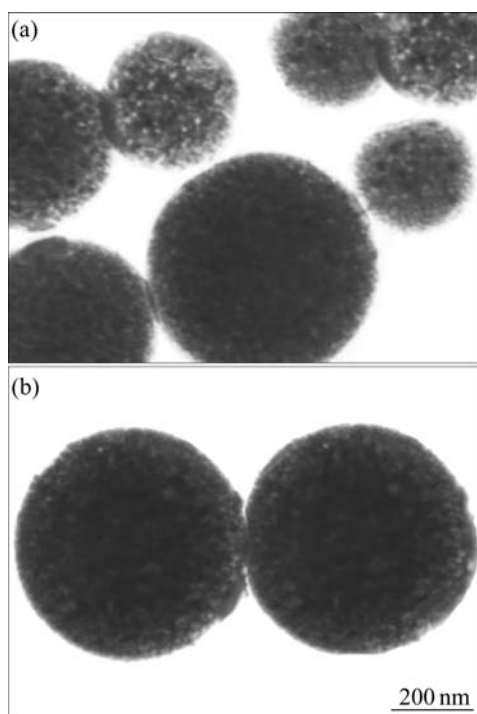
Fig.6 TEM images of powders prepared from solution with various concentrations (pyrolysis temperature: 800 ℃): (a) 0.05 mol/L; (b) 0.4 mol/L

the action of electron (e⁻) and hole (h⁺), TiO₂ photocatalysts can decompose many organic compounds. The photocatalytic activity of TiO_2 is related to the generation capacity of electrons and holes, the separation efficiency of the photogenerated charge pair, and the transfer efficiency of holes and electrons to compounds absorbed on TiO_2[9]. The yield of the photogenerated electron-hole pair mainly depends on the intensity of incident photons with energy exceeding or equaling the TiO_2 band gap energy. In order to check the effect of process parameters on titania band gap energy, the optical property of doping titania was investigated by

UV-vis transmission spectrometry. Fig.7 shows the UV-vis absorption spectra of the doping titania. It can be seen from Fig.7 that the pyrolysis temperature has a small effect on the spectra of doping titania powders. The absorption edge of doping titania powder was between 385 nm (3.22 eV) and 383 nm (3.24 eV). These values are very close to those of anatase TiO_2 (3.2 eV), indicating that silver doping did not cause any significant shift on the fundamental absorption edge of titania.
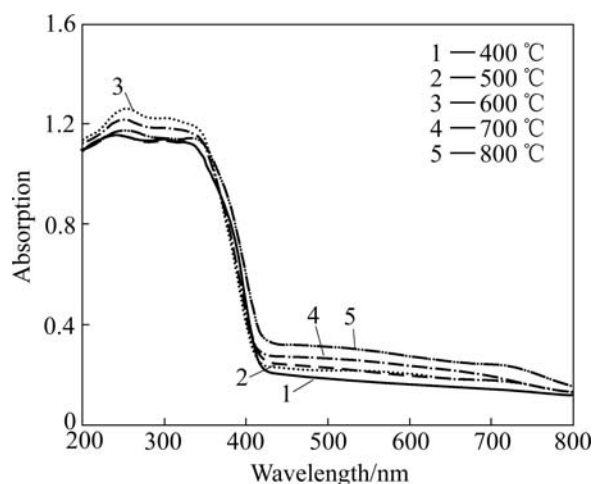

Fig.7 UV-vis absorption spectra of doping powders prepared at different pyrolysis temperatures

3.4 Property of ion release

The antibacterial activity of doping TiO_2 is closely related to the concentrations of silver ion or other ion around the surface of the specimen[10]. It is known that antibacterial material exhibits stronger antibacterial activity as it releases more silver ion into water. However, the release of excessive ions may shorten the life of antibacterial material and contaminate the environment, thus the rate of ion release of doping titania powders attracts many attention.

Fig.8 shows the concentration of F^- and Ag^+ in the supernatants collected from water containing composite. It can be seen that the pyrolysis temperature has a significant effect on the ion release of doping titania powders. The amount of fluorine and silver ions released decreases dramatically with increasing the pyrolysis temperature. The concentration of fluorine ion released decreases from 145.3 to 30.5 mg/L and the concentration of silver ion released decreases from 58.2 to 33.8 mg/L as the pyrolysis temperature increases from 400 ℃ to 500 ℃. A lot of fluorine ions released from composite powder prepared at 400 ℃ are attributed to the $TiOF_2$ formed in powder. A large amount of silver ions released are due to the fact that fluorine ions are capable of dissolving composite released in water. When the pyrolysis temperature is above 500 ℃, there is slight

difference between the concentration of fluorine ions and silver ions released from the powders in spite of the change of heating temperature.
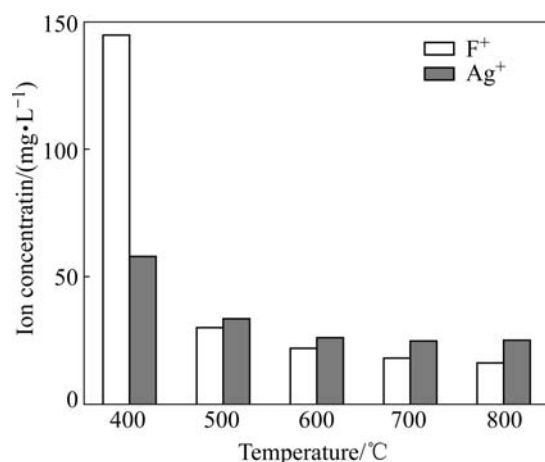
Fig.8 Effect of pyrolysis temperature on ion release property of doping TiO_2 powers

3.5 Antibacterial activity

The minimum inhibitory concentration of doping TiO_2 powder prepared at various temperatures is listed in Table 1. The MIC of doping TiO_2 powder is smaller than the standard MIC value of Japanese antibacterial material (800 mg/L), which indicates that the composite powder has stronger antibacterial activity against *E.coli.* The MIC of doping TiO_2 powder increases with increasing the pyrolysis temperature, which means that the antibacterial activity decreases with increasing the pyrolysis temperature. The decrease of antibacterial activity is contributed to the decrease of ion release of composite. Ionic silver has the highest and broad-spectrum antibacterial activity among metal ions. It adsorbs the protein on the surface of the bacterial membrane, influencing membrane synthesis with S—Ag bonds[11], inhibits the DNA synthesis with direct binding on the bacterial DNA and finally results in the death of bacteria[12]. So the amount of silver ions released from materials is considered as one of the most important factors in evaluating its antibacterial activity. It can be seen from Table 1 that the MICs of doping TiO_2 powder prepared at 400, 500, 600, 700 and 800 ℃ are 2.0, 6.0, 7.5, 8.5 and 9.0 mg/L, respectively, from which the concentrations of silver ion calculated are 11.6, 20.3, 19.8, 21.3 and 22.8 mg/L, respectively. The amount of silver ions released from powders prepared at 400 ℃ is less than that prepared above 500 ℃. This indicates that fluorine ions released from powder show antibacterial activity against *E.coli* as well. Fluorine ions with antibacterial effect against oral bacteria have been reported in previous researches and fluoride-releasing composite is used as a highly elective anticaries agent in dental fields. There are two possible explanations for

antibacterial mechanism of the fluorine ions[13]. One is that fluorine ions can affect bacterial metabolism as an enzyme inhibitor, and the other is that metal-fluoride complexes are responsible for fluoride inhibition of proton-translocating F-AT-Pases and mimicking phosphate to form complexes with ADP at the reaction centers of the enzymes[14].

Table 1 MIC of doping TiO_2 powders against *E.coli*

Pyrolysis temperature/℃	MIC of powder/$(mg·L^{-1})$
400	2.0
500	6.0
600	7.5
700	8.5
800	9.0

The antibacterial activity of titania has also been reported in the biomedical fields. The antibacterial mechanism of titania is that the reactive oxygen species generated by titania photocatalytic reactions promoted peroxidation of the polyunsaturated phospholipids component of the lipid membrane, induced major disorder in the bacteria and caused various damages to living organism when TiO_2 was illuminated in UV light [15−16]. Then, organic compounds were decomposed and mineralized by participating in a series of oxidation reactions leading to carbon dioxide.

4 Conclusions

1) Spherical doping titania composite powders were synthesized by spray pyrolysis from an aqueous solution containing H_2TiF_6 and $AgNO_3$. The particle size of powder can be controlled by adjusting the concentration of solution. Both the particle size and the value of standard deviation of particle size increase with the increase of the titanic concentration.

2) The pyrolysis temperature has a significant effect on the properties of composite powder. $TiOF_2$ is obtained in composite when the pyrolysis temperature is 400 ℃. With increasing the pyrolysis temperature from 400 to 800 ℃, the crystal size of titania increases from 14.1 to 26.5 nm. The amount of ion released from powder decreases with increasing the pyrolysis temperature. But the optical property of doping titania powders is not affected by the pyrolysis temperature.

3) Antibacterial test results show that both silver ion and fluorine ion released from powder play an antibacterial role against bacteria, and the antibacterial activity of composite powder against *E.coli* is strengthened with the increase of the content of silver ion and fluorine ion.

References

[1]   BARTKOVA H, KLUSON P, BARTEK L, DROBEK M, CAJTHAML T, KRYSA J. Photoelectrochemical and photocatalytic properties of titanium (IV) oxide nanoparticulate layers [J]. Thin Solid Films, 2007, 515(24): 8455−8460.

[2]   VICENTE G S, MORALES A, GUTIERREZ M T. Sol-gel TiO$_2$ antireflective films for textured monocrystalline silicon solar cells [J]. Thin Solid Films, 2002, 403(1): 335−338.

[3]   LI C P, WANG J F, SU W B, CHEN H C, WANG Y J, ZHUANG D X. Effect of sinter temperature on the electrical properties of TiO$_2$-base capacitor-varistors [J]. Materials Letter, 2003, 57: 1400−1405.

[4]   VERRAN J, SANDOVAL G, ALLEN N S, EDGE M, STRATTON J. Variables affecting the antibacterial properties of nano and pigmentary titania particles in suspension [J]. Dyes and Pigments, 2007, 73(3): 298−304.

[5]   SOKMEN M, OZKAN A. Decolourising textile wasterwater with modified titania: The effects of inorgania anions on the photocatalysis [J]. Journal of Photochemistry and Photobiology A: Chemistry, 2002, 147(1): 77−81.

[6]   HE Chao, YU Yun, HU Xing-fang, ANDRE L. Influence of silver doping on the photocatalytic activity of titania films [J]. Applied Surface Science, 2002, 200(1/4): 239−247.

[7]   LIN F, NOBUYUKI I, SHOGO S, TAKAYOSHI U. Preparation of Au/TiO$_2$ catalysts by suspension spray reaction method and their catalytic property for CO oxidation [J]. Applied Catalysis A: General, 2003, 246(1): 87−95.

[8]   GAUDON M, DJURADO E, MENZLER N H. Morphology and sintering behaviour of yttria stabilised zirconia (8-YSZ) powders synthesised by spray pyrolysis [J]. Ceramics International, 2004, 30(8): 2295−2303.

[9]   CHEN Shi-Fu, LIU Yun-Zhang. Study on the photocatalytic degradation of glyphosate by TiO$_2$ photocatalyst [J]. Chemosphere, 2007, 67(5): 1010−1017.

[10]   KUMAR R, MUNSTEDT H. Silver ion release from antimicrobial polyamide/silver composites [J]. Biomaterials, 2005, 26(14): 2081−2088.

[11]   PENG Bing, YUAN Chun, WEI Shun-wen, YU Yan-fen, SU Wei-feng. Preparation of titanium dioxide/silver sulfate powder and its antibacterial activity [J]. Trans Nonferrous Metals Soc China, 2005, 15(5): 1156−1160.

[12]   FENG Q L, WU J, CHEN G Q, CUI F Z, KIM T N, KIM J O. A mechanistic study of the antibacterial effect of silver ions on *E.coli* and staphylococcus aureus [J]. J Biomed Mater Res, 2000, 52: 662−668.

[13]   ISHIHARA M, KOSAKA T, NAKAMURA T, TSUGAWA K, HASEGAWA M, KOKAI F, KOGA Y. Antibacterial activity of fluorine incorporated DLC films [J]. Diamond and Related Materials, 2006, 15(4/8): 1011−1014.

[14]   KRISHNAN S, WARD R J, HEXEMER A, SOHN K E, LEE K L, ANGERT E R, FISCHER D A, KRAMER E J, OBER C K. Surfaces of fluorinated pyridinium block copolymers with enhanced antibacterial activity [J]. Langmuir, 2006, 22(26): 11255−11266.

[15]   MANESS P C, SMOLINSKI S L, BLAKE D M, HUANG Z, WOLFRUM E J, JACOBY W A. Bactericidal activity of photocatalytic TiO$_2$ reaction: Toward an understanding of its killing mechanism [J]. Appl Environ Microbiol, 1999, 65(9): 4094−4098.

[16]   HUANG Z, MANESS P C, BLAKE D M, WOLFRUM E J, SMOLINSKI S L, JACOBY W A. Bactericidal mode of titanium dioxide photocatalysis [J]. Photochem and Photobiol A: Chem, 2000, 130: 163−170.

(Edited by LI Xiang-qun)